# Repulsive DNA-DNA Interactions Accelerate Viral DNA Packaging in Phage Phi29

Nicholas Keller,[1] Damian delToro,[1] Shelley Grimes,[2] Paul J. Jardine,[2] and Douglas E. Smith[1]
[1]Department of Physics, University of California, San Diego, 9500 Gilman Dr., La Jolla, California 92093, USA
[2]Department of Diagnostic and Biological Sciences and Institute for Molecular Virology, University of Minnesota, 515 Delaware Street SE, Minneapolis, Minnesota 55455, USA
(Received 27 February 2014; published 17 June 2014)

We use optical tweezers to study the effect of attractive versus repulsive DNA-DNA interactions on motor-driven viral packaging. Screening of repulsive interactions accelerates packaging, but induction of attractive interactions by spermidine$^{3+}$ causes heterogeneous dynamics. Acceleration is observed in a fraction of complexes, but most exhibit slowing and stalling, suggesting that attractive interactions promote nonequilibrium DNA conformations that impede the motor. Thus, repulsive interactions facilitate packaging despite increasing the energy of the theoretical optimum spooled DNA conformation.

DOI: 10.1103/PhysRevLett.112.248101 PACS numbers: 87.14.gk, 05.70.Ln, 87.15.-v, 87.80.Cc

In the assembly of many viruses, molecular motors provide the driving forces to package DNA to near crystalline densities inside preassembled viral proheads [1–5]. The DNA, a negatively charged, semiflexible polymer, is compacted to such high density that its bending rigidity, electrostatic self-repulsion, and entropy loss present a strong barrier to confinement [6–15]. Measurements show that viral molecular motors can exert high forces (>60 pN) and translocate DNA at rates ranging from ~100–2000 base pairs/sec [1,7,16,17]. The rate of packaging decreases with increasing prohead filling due, in part, to the buildup of large forces resisting DNA confinement [18,19]. In addition to being of biological interest, viral DNA packaging is a unique model for investigating and understanding the behavior of polymers under nanoscale confinement, which has long been a topic of interest in polymer physics [20,21].

Positively charged polyamines such as spermidine$^{3+}$, present in the cells viruses infect, are thought to play an important role in packaging by screening the DNA charge [12,22,23]. Above a critical concentration, polyamines can induce a phase transition where the DNA-DNA interaction changes from purely repulsive to partly attractive, which causes free DNA in solution to condense into a tight spool, a conformation similar to that proposed to occur in viruses [6,10,12,23-27].

The effect of repulsive versus attractive DNA-DNA interactions has been considered in many theoretical studies and all have predicted that attractive interactions would facilitate DNA packaging by reducing the forces resisting DNA confinement. In Brownian dynamics simulations, Kindt *et al.* predicted arrangement of the DNA into a toroid-shaped spool that evolved into an inverse coaxial spool [8]. With a purely repulsive interaction, a more disordered structure and higher resistance forces were predicted, although it was hypothesized that the DNA would eventually equilibrate to a spool conformation. Kindt *et al.*, Tzlil *et al.*, and Purohit *et al.* developed continuum-mechanics theories that assume the DNA is packaged into a minimum-energy spool conformation with local hexagonal packing [8,10–12]. These models reproduce many of the experimental trends in DNA packaging and ejection, including the sharp increase in resistance towards the end of packaging. With an attractive potential, ~10 × lower resistance is predicted than with a purely repulsive one [12].

In Langevin dynamics simulations with an attractive potential, Forrey and Muthukumar predicted increased DNA ordering and structures resembling a folded toroid [14]. They also predicted that nonequilibrium dynamics would cause heterogeneity in the DNA conformations and packaging forces. Similar effects were predicted with purely repulsive interactions [13–15]. In molecular dynamics simulations, Petrov and Harvey predicted sharply reduced packaging forces with attractive interactions and toroidal DNA conformations with a central void [28]. In Monte Carlo simulations, Comolli *et al.* predicted heterogeneous conformations with DNA occupying the entire prohead with uniform average density [29].

Here, we report experimental studies of the effect of attractive versus repulsive DNA-DNA interactions on viral DNA packaging dynamics in bacteriophage phi29, in which a 19.3 kilo-base-pair genome (6.6 $\mu$m) is translocated into a 54 × 42 nm prohead [5]. We use optical tweezers to directly measure packaging of single DNA molecules into single phi29 proheads in real time in three different conditions: (1) a standard packaging buffer in which the DNA is screened mainly by $Na^+$ and $Mg^{2+}$ ions (purely repulsive regime); (2) a low concentration of spermidine, in which the repulsion is nearly maximally screened; and (3) a high concentration of spermidine, in which the interaction becomes partly attractive. We find that screened repulsive DNA-DNA interactions facilitate efficient viral packaging despite increasing the energy of the close-packed DNA conformation.

Proheads were prepared as described previously and recombinant motor protein, gp16, was prepared in *E. Coli*,

 

using a SUMO tag [30,31]. We used a 25 339 bp dsDNA construct, biotin labeled at one end, prepared by polymerase chain reaction from $\lambda$–DNA with no terminal proteins [32]. Measurements were made at ~23 °C in the standard condition (25 m$M$ Tris-HCl, $p$H 7.5, 50 m$M$ NaCl, 5 m$M$ $MgCl_2$, 0.05 mg/ml BSA, and 0.5 m$M$ ATP) and with added spermidine trihydrochloride.

We determined that the threshold for DNA condensation was ~1 m$M$ spermidine by conducting DNA force-extension measurements. We chose a "low spermidine" concentration of 0.8 m$M$, yielding purely repulsive interactions with near maximum screening, indicated by the force increasing monotonically with extension [26]. We chose a "high spermidine" concentration of 5 m$M$, where we observed nonmonotonic, "stick-slip" force-extension behavior, indicating attractive DNA-DNA interactions [26]. A similar spermidine concentration is reported in host cells (~10 m$M$) [24], although the amount bound to viral DNA *in vivo* is unknown and depends on partitioning in the cell and binding of other ions and proteins.

Measurements of DNA packaging were made using optical tweezers techniques similar to those described previously [18,19,33,34]. These techniques provide details on the packaging dynamics not available from bulk assays and permit measurements in condensing conditions, which are problematic in bulk due to DNA aggregation and interference with DNA digestion by DNAse. Briefly, prohead-motor complexes are attached to one microsphere and DNA molecules are attached to a second microsphere. The DNA molecule is brought into the reaction buffer containing ATP and spermidine, and then, within a few seconds, is brought into contact with the motor to initiate packaging [Fig. 1(a)]. We note that the prohead is permeable to water and small ions including spermidine [35,36]. Measurements in the standard condition and with low spermidine (maximum screening) with a small (5 pN) applied force showed fairly uniform packaging trajectories [Fig. 1(b)]. However, with low spermidine, the average packaging rate and motor velocity (translocation rate not including pauses and slips, as discussed previously [7,18,19]) are higher than in the standard condition across the whole range of filling levels [Figs. 2(a) and 2(b)].

The motor velocity in low spermidine also exhibits a plateau up to ~30% filling [Fig. 2(b)]. In this low-filling regime, additional measurements show that the velocity decreases with increasing applied force [Fig. 3(a)]. Together these measurements indicate that there is almost no resistance to packaging in this regime, because no slowing was observed. The higher motor velocity measured with low spermidine [Fig. 2(b)] is thus not due to a reduced resistance to packaging, but rather indicates that spermidine acts directly on the motor to increase its velocity, presumably by directly affecting the motor protein structure and/or protein-DNA interactions [37,38].

Previous studies employed the measured velocity versus applied force relationship to infer an effective "internal force" resisting packaging [7,18,19]. However, recent studies indicate that although both prohead filling and applied force slow the motor, they have a different influence on the motor kinetics and cannot be directly equated [39,40]. In the present Letter, we refer to "resistance" or "load" on the motor as any interaction between the packaged DNA and motor which slows packaging.

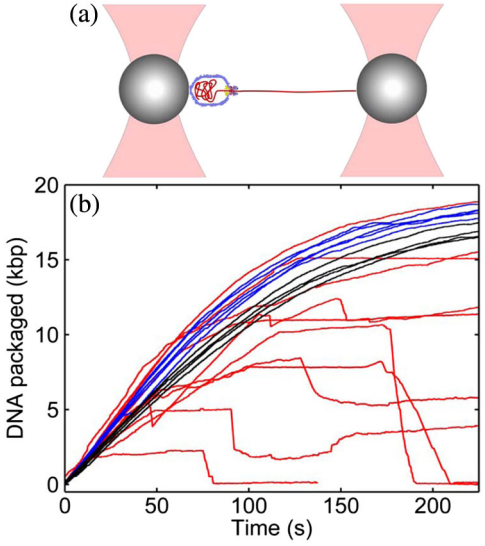


FIG. 1 (color online). (a) The prohead-motor complex is attached to one optically trapped microsphere (left) and the end of the DNA is attached to a second trapped microsphere (right). (b) Typical measurements with 5 pN external load in the standard condition (black), low spermidine (blue, slightly faster), and high spermidine (red, highly heterogeneous).

With low spermidine, the motor velocity remains higher as the filling increases than in the standard condition, consistent with an expected reduction in packing force due to increased screening [8,12,14,18]. Thus, low spermidine accelerates packaging by directly increasing motor velocity and decreasing the load on the motor. The latter finding is consistent with theoretical studies which predict that increased screening would facilitate packaging by reducing the energy needed for DNA confinement [10,12,14,28].

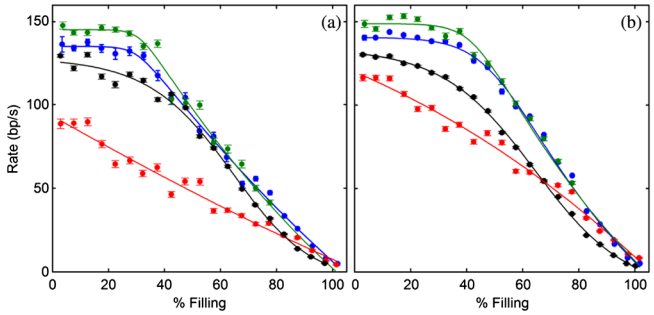


FIG. 2 (color online). (a) Average packaging rate and (b) motor velocity (packaging rate not including pauses and slips) versus prohead filling under 5 pN applied force in the standard condition (black, 3rd highest initial rate), low spermidine (blue, 2nd highest initial rate), high spermidine (red, lowest initial rate), and for the subset of complexes in high spermidine that package to > 80% filling (green, highest initial rate).

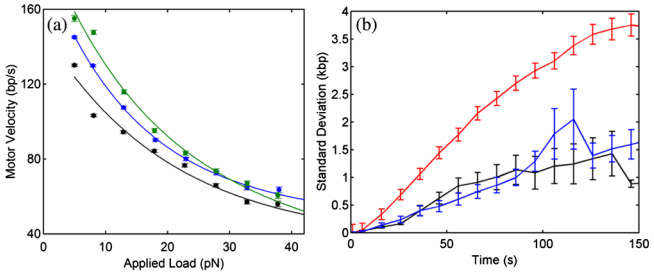


FIG. 3 (color online). (a) Average motor velocity versus applied load for complexes that reached >30 pN with <20% filling in the standard condition (black, N = 113 events, lowest rates), low spermidine (blue, N = 61), and fast (nonstalling) complexes in high spermidine (green, N = 101, highest rates). (b) Standard deviation in DNA length packaged by different complexes for the standard condition (black), low spermidine (blue, nearly equal to standard), and high spermidine (red, highest values) under 5 pN load.

The behavior observed with an attractive interaction with high spermidine is dramatically different [Fig. 1(b)]. Large heterogeneity is observed in the dynamics of different individual complexes, characterized by a significant increase in standard deviation of packaged DNA lengths with time [Fig. 3(b)]. Events in which the motor stalled were often observed: 51% (N = 149) of complexes stalled at <50% filling versus only 12% (N = 18) in the standard condition and 15% in low spermidine (N = 37). This observed inhibition was not anticipated by any of the theoretical modeling studies.

Compared with the standard and low spermidine conditions, the average packaging rate with high spermidine is sharply reduced, except for events which reached ~80% filling [Fig. 2(a)]. 75% of complexes stall before reaching this point (N = 220). However, the 25% of complexes that reach 80% filling have a significantly higher average motor velocity across the entire range of fillings [Fig. 2(b)]. The behavior of this "fast subset" is consistent with theoretical predictions that attractive interactions would enhance packaging. These complexes exhibit less pausing and slipping as well as higher motor velocity. The motor velocity exhibits a similar but slightly higher velocity plateau up to ~30% filling as in the standard condition. This plateau implies there is negligible resistance up to ~30% filling and that high spermidine increases the motor velocity more than low spermidine.

However, 75% of complexes are inhibited by high spermidine and the average motor velocity for the entire ensemble with high spermidine is much lower than with low spermidine [Fig. 2(b)] and shows a shorter plateau up to only ~10% filling. This suggests that attractive interactions cause, on average, an increase in resistance faced by the motor even at fillings as low as 10%, contrary to predictions which assume a minimum-energy spooled DNA configuration. In addition to decreasing the motor velocity, high spermidine also causes an increase in motor pausing and slipping. There is a 12-fold increase in percent time spent paused at <50% filling (N = 293 events) versus a 1.4-fold increase with low spermidine (N = 249). Slips are 3× more frequent (N = 5609) and 4.7× longer on average (2480 ± 200 bp) than in the standard condition versus 1.2× more frequent and 1.1× longer in low spermidine (N = 1914). Also, 53% of slips (N = 2947) occurred at <50% filling versus 10% in the standard condition (N = 98) and 11% in low spermidine (N = 216). These observations show that in the presence of attractive DNA-DNA interactions, the load faced by the motor in individual proheads is widely variable and often high enough to cause stalling.

We considered whether the inhibition might be due to a direct effect of spermidine on the motor rather than an effect on the packaged DNA conformation. Two observations suggest this is not the case. First, for the subset of fast complexes, high spermidine increases the inherent motor velocity at low filling more than low spermidine [Fig. 2(b)]. Second, we observe a small fraction of events in which packaging does not show the usual trend of slowing down and the length of DNA translocated greatly exceeds 100% of the genome length. We interpret these events as cases where the prohead is perforated such that the DNA leaks out of the prohead and thus the motor faces no resistance. A similar effect was observed in previous studies of phage lambda packaging with proheads lacking a stabilizing protein essential in that system [16]. These events provide evidence that high spermidine does not directly inhibit the motor because they displayed higher velocity (155 bp/s average, N = 32) while translocating the full genome length than in the standard condition (130 bp/s, N = 35). Also, the perforated-head events (exhibiting no slowing) in high spermidine exhibit ~140-fold less-frequent pausing and ~80-fold less-frequent slipping than regular events.

Although a 5 pN force was applied to keep the DNA stretched during measurements, this is insufficient to completely prevent DNA condensation [26]. In control experiments with tethered DNA, slight shortening of the DNA extension was observed (6 bp/s on average), suggesting that small sections of the unpackaged DNA tether condense during packaging. To investigate whether such condensation interferes with translocation, we conducted several experiments.

First, we performed measurements with high spermidine in which we relaxed the DNA to near-zero tension during packaging to promote condensation of external DNA [Fig. 4(a)]. The DNA was then stretched to 5 pN, revealing shortening of the extension due to partial condensation. We found that such condensation did not significantly affect the motor as 90% (N = 45) of these complexes continued packaging without interruption, indicating that the motor can usually exert sufficient force to unravel sections of condensed DNA. Second, we conducted experiments in which, upon observing stalling of a complex, we ramped the force from 5 pN to 25 pN to decondense any unpackaged DNA [Fig. 4(b)]. This did not enable any of the stalled complexes to resume packaging (N = 25). Ramping to 25 pN in the standard conditions does not halt packaging

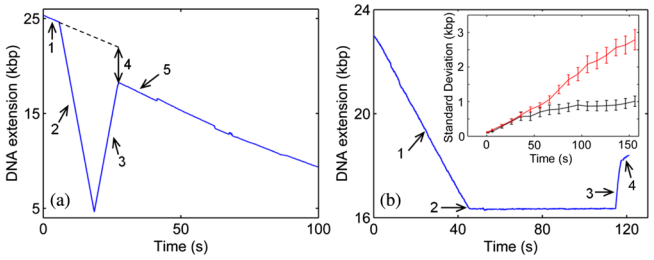


FIG. 4 (color online). (a) Example where a complex was packaging under 5 pN applied load (shortening of the DNA extension; section no. 1) and was relaxed to bring the applied force to near zero (section no. 2). The DNA was then stretched again to 5 pN (no. 3) and found to be partly condensed (indicated by 4) (dashed line shows the expected trend for packaging in the absence of condensation). Despite condensation, packaging continued (no. 5). (b) Example in which motor was packaging under 5 pN load (no. 1) and then stalled (no. 2). The DNA was then stretched to 25 pN to extend any condensed segments (no. 3), but no recovery in packaging was observed (no. 4). Inset shows standard deviation in lengths measured at 15 pN in the standard condition (black, lower values) and high spermidine (red, higher values).

[Fig. 3(a)]. Third, we conducted packaging measurements with a 15 pN constant applied force, high enough to prevent DNA condensation [26]. Although this force slows the motor, it does not eliminate the increase in heterogeneity caused by spermidine [Fig. 4(b), inset].

Since our experiments show that the increased heterogeneity observed with high spermidine is not due to direct alteration of motor function and not due to condensation of the unpackaged DNA, we conclude that it is due to heterogeneity in the load on the motor presented by varying conformations of the packaged DNA. We interpret these findings as indicating that DNA molecules packaged in individual proheads adopt widely different nonequilibrium conformations, often including highly unfavorable jammed conformations that impede the motor. Our findings further suggest that attractive DNA-DNA interactions exaggerate the formation of these nonequilibrium conformations. A small fraction of complexes in which the DNA adopts a nearer-to-equilibrium conformation package faster than in purely repulsive conditions, but in the majority the DNA is kinetically trapped in highly unfavorable nonequilibrium conformations that stall packaging. Our results indicate that repulsive DNA-DNA interactions play an important role in facilitating viral packaging by mitigating the formation of such conformations.

Our finding of faster packaging with low spermidine is consistent with models which predict that increased screening of DNA should reduce the forces resisting packaging [6,8,10,12,14] and studies showing that osmotic pressures required to inhibit ejection are reduced in conditions with increased screening [36]. However, our findings of strong inhibition with high spermidine are different than were anticipated. Studies with condensing levels of spermine$^{4+}$ found inhibition of DNA ejection by phages T5 and lambda, whereas it is complete in the absence of polyamines [9,36,41]. Those studies indicate that condensation reduces the ejection force, suggesting that they would decrease the force resisting packaging. This notion is consistent with our finding of accelerated packaging in a small fraction of complexes, but inconsistent with our finding that the packaging is stalled in the majority of complexes. Thus, our studies imply that DNA does not generally follow the reverse conformational trajectory during ejection that is followed during packaging.

Modeling studies that incorporated attractive DNA-DNA interactions predict more ordered structures and lower forces resisting DNA confinement. The likely explanation is that these studies have considered equilibrated DNA conformations. In continuum models, packaging is assumed to be a quasistatic process in which the DNA continually relaxes to a free-energy minimum conformation [8,10–12,42]. As discussed by Tzlil *et al.*, the forces resisting packaging may be higher than the calculated statistical-thermodynamic force due to dynamic dissipative effects [10]. In most packaging simulations, the DNA is periodically equilibrated [8,14,43], subject to limits on simulation time. Several studies observed effects attributable to nonequilibrium dynamics, including heterogeneous DNA conformations, fluctuating packaging forces, pausing in packaging, and higher forces resisting packaging than driving DNA ejection [13–15]. However, none of these studies predicted strong inhibition at low filling and none specifically addressed the effect of attractive versus repulsive interactions on nonequilibrium effects.

Recent electron microscopy studies investigated condensation of DNA in phage T5 in which spermine$^{4+}$ was added after DNA was partly ejected [44]. Toroids with outer radii as small as ~25 nm were observed, smaller than the ~80 nm prohead diameter of T5 and ~42 nm diameter of phi29. The subset of fast complexes we observe with high spermidine may correspond to cases where the DNA is able to condense into small toroids that present little resistance to confinement (though evidently not zero resistance, as the motor does progressively slow above ~30% filling).

A potentially related effect has been observed in simulations of DNA condensation inside proheads where DNA-DNA interactions were switched from repulsive to attractive after partial packaging. Kinetically trapped nonequilibrium conformations that do not relax to toroids were predicted even at prohead fillings as low as 30% [28]. Although such conformations were not observed in continuous packaging simulations with constant attractive interactions, related effects likely cause the inhibition we observe. Notably, studies of free DNA condensation have reported conformational changes on time scales ranging from tens of minutes to hours [45,46].

In summary, we report that low concentrations of spermidine, resulting in a maximally screened repulsive DNA-DNA interaction, accelerate DNA packaging by both stimulating the motor function directly and reducing the load on the motor that builds with increased prohead filling. In contrast, a high concentration of spermidine, which induces

an attractive DNA-DNA interaction, results in highly heterogeneous dynamics. A small fraction of complexes package faster than in the purely repulsive condition, but the majority of complexes exhibit dramatic slowing, pausing, and stalling at low filling, which we attribute to formation of highly nonequilibrium DNA conformations. Our results indicate that repulsive DNA-DNA interactions play an important role in facilitating efficient viral packaging despite increasing the energy of the close-packed DNA conformation.

We thank Zachary Berndsen, Mariam Ordyan, and Al Schweitzer for advice and assistance. This research was supported by NSF Grant No. PHY-0848905 and NIH Grant No. R01-GM088186.

*Note added in proof.*—In a recently published article [47] we have additionally shown that the DNA at 75% filling undergoes nonequilibrium dynamics with a slow relaxation time of $> 10$ minutes even with purely repulsive DNA-DNA interactions; however this does not cause dramatic stalling of the motor as we report here with attractive interactions.

[1] D. E. Smith, Curr. Opin. Virol. **1**, 134 (2011).
[2] X. Qiu, D. C. Rau, V. A. Parsegian, L. T. Fang, C. M. Knobler, and W. M. Gelbart, Phys. Rev. Lett. **106**, 028102 (2011).
[3] S. R. Casjens, Nat. Rev. Microbiol. **9**, 647 (2011).
[4] Y. R. Chemla and D. E. Smith, *Single-Molecule Studies of Viral DNA Packaging* (Springer, New York, 2012), p. 549.
[5] M. C. Morais, *The dsDNA Packaging Motor in Bacteriophage ϕ29* (Springer, New York, 2012), p. 511.
[6] S. C. Riemer and V. A. Bloomfield, Biopolymers **17**, 785 (1978).
[7] D. E. Smith, S. J. Tans, S. B. Smith, S. Grimes, D. L. Anderson, and C. Bustamante, Nature (London) **413**, 748 (2001).
[8] J. Kindt, S. Tzlil, A. Ben-Shaul, and W. M. Gelbart, Proc. Natl. Acad. Sci. U.S.A. **98**, 13671 (2001).
[9] A. Evilevitch, L. Lavelle, C. M. Knobler, E. Raspaud, and W. M. Gelbart, Proc. Natl. Acad. Sci. U.S.A. **100**, 9292 (2003).
[10] S. Tzlil, J. T. Kindt, W. M. Gelbart, and A. Ben-Shaul, Biophys. J. **84**, 1616 (2003).
[11] P. K. Purohit, J. Kondev, and R. Phillips, Proc. Natl. Acad. Sci. U.S.A. **100**, 3173 (2003).
[12] P. K. Purohit, M. M. Inamdar, P. D. Grayson, T. M. Squires, J. Kondev, and R. Phillips, Biophys. J. **88**, 851 (2005).
[13] I. Ali, D. Marenduzzo, and J. M. Yeomans, Phys. Rev. Lett. **96**, 208102 (2006).
[14] C. Forrey and M. Muthukumar, Biophys. J. **91**, 25 (2006).
[15] S. C. Harvey, A. S. Petrov, B. Devkota, and M. B. Boz, Phys. Chem. Chem. Phys. **11**, 10553 (2009).
[16] D. N. Fuller, D. M. Raymer, J. P. Rickgauer, R. M. Robertson, C. E. Catalano, D. L. Anderson, S. Grimes, and D. E. Smith, J. Mol. Biol. **373**, 1113 (2007).
[17] D. N. Fuller, D. M. Raymer, V. I. Kottadiel, V. B. Rao, and D. E. Smith, Proc. Natl. Acad. Sci. U.S.A. **104**, 16868 (2007).
[18] D. N. Fuller, J. P. Rickgauer, P. J. Jardine, S. Grimes, D. L. Anderson, and D. E. Smith, Proc. Natl. Acad. Sci. U.S.A. **104**, 11245 (2007).
[19] J. P. Rickgauer, D. N. Fuller, S. Grimes, P. J. Jardine, D. L. Anderson, and D. E. Smith, Biophys. J. **94**, 159 (2008).
[20] P. G. De Gennes, *Scaling Concepts in Polymer Physics* (Cornell University Press, Ithaca, 1979).
[21] W. Reisner, J. N. Pedersen, and R. H. Austin, Rep. Prog. Phys. **75**, 106601 (2012).
[22] D. C. Rau and V. A. Parsegian, Biophys. J. **61**, 246 (1992).
[23] V. A. Bloomfield, Biopolymers **44**, 269 (1997).
[24] J. Pelta, F. Livolant, and J. Sikorav, J. Biol. Chem. **271**, 5656 (1996).
[25] M. E. Cerritelli, N. Q. Cheng, A. H. Rosenberg, C. E. McPherson, F. P. Booy, and A. C. Steven, Cell **91**, 271 (1997).
[26] C. G. Baumann, V. A. Bloomfield, S. B. Smith, C. Bustamante, M. D. Wang, and S. M. Block, Biophys. J. **78**, 1965 (2000).
[27] N. V. Hud and I. D. Vilfan, Annu. Rev. Biophys. Biomol. Struct. **34**, 295 (2005).
[28] A. S. Petrov and S. C. Harvey, J. Struct. Biol. **174**, 137 (2011).
[29] L. R. Comolli, A. J. Spakowitz, C. E. Siegerist, P. J. Jardine, S. Grimes, D. L. Anderson, C. Bustamante, and K. H. Downing, Virology **371**, 267 (2008).
[30] R. J. Peroutka III, S. J. Orcutt, J. E. Strickler, and T. R. Butt, *SUMO Fusion Technology for Enhanced Protein Expression and Purification in Prokaryotes and Eukaryotes* (Springer, New York, 2011), p. 15.
[31] W. Zhao, M. C. Morais, D. L. Anderson, P. J. Jardine, and S. Grimes, J. Mol. Biol. **383**, 520 (2008).
[32] D. N. Fuller, G. J. Gemmen, J. P. Rickgauer, A. Dupont, R. Millin, P. Recouvreux, and D. E. Smith, Nucleic Acids Res. **34**, e15 (2006).
[33] J. P. Rickgauer, D. N. Fuller, and D. E. Smith, Biophys. J. **91**, 4253 (2006).
[34] D. delToro and D. E. Smith, Appl. Phys. Lett. **104**, 143701 (2014).
[35] M. C. Morais, S. Kanamaru, M. O. Badasso, J. S. Koti, B. A. Owen, C. T. McMurray, D. L. Anderson, and M. G. Rossmann, Nat. Struct. Mol. Biol. **10**, 572 (2003).
[36] A. Evilevitch, L. T. Fang, A. M. Yoffe, M. Castelnovo, D. C. Rau, V. A. Parsegian, W. M. Gelbart, and C. M. Knobler, Biophys. J. **94**, 1110 (2008).
[37] C. A. Panagiotidis, S. Artandi, K. Calame, and S. J. Silverstein, Nucleic Acids Res. **23**, 1800 (1995).
[38] A. A. Ouameur, E. Mangier, S. Diamantoglou, R. Rouillon, R. Carpentier, and H. Tajmir-Riahi, Biopolymers **73**, 503 (2004).
[39] G. Chistol, S. Liu, C. L. Hetherington, J. R. Moffitt, S. Grimes, P. J. Jardine, and C. Bustamante, Cell **151**, 1017 (2012).
[40] S. Liu, G. Chistol, C. Hetherington, S. Tafoya, K. Aathavan, J. Schnitzbauer, S. Grimes, P. Jardine, and C. Bustamante, Cell **157**, 702 (2014).
[41] M. De Frutos, S. Brasiles, P. Tavares, and E. Raspaud, Eur. Phys. J. E **17**, 429 (2005).
[42] W. Klug and M. Ortiz, J. Mech. Phys. Solids **51**, 1815 (2003).
[43] A. S. Petrov and S. C. Harvey, Structure **15**, 21 (2007).
[44] A. Leforestier and F. Livolant, Proc. Natl. Acad. Sci. U.S.A. **106**, 9157 (2009).
[45] S. A. Allison, J. C. Herr, and J. M. Schurr, Biopolymers **20**, 469 (1981).
[46] I. D. Vilfan, C. C. Conwell, T. Sarkar, and N. V. Hud, Biochemistry **45**, 8174 (2006).
[47] Z. T. Berndsen, N. Keller, S. Grimes, P. J. Jardine, and D. E. Smith, Proc. Natl. Acad. Sci. U.S.A. **111**, 8345 (2014).